Modulation of 1FGL J1018.6−5856 VHE γ-ray light-curves due to γ-γ absorption under different orbital parameters

Author: Pere Gironella Gironell.
Facultat de Física, Universitat de Barcelona, Diagonal 645, 08028 Barcelona, Spain.

Advisor: Marc Ribó Gomis

Abstract: Binary systems composed of a neutron star or a black hole, and emitting in very high energy (VHE) γ-rays, have attracted a lot of interest in the last decade. One of these systems, 1FGL J1018.6−5856, is known to be composed of massive star of spectral type O6V((f)) and has an orbital period of 16.58 days, from the periodic emission in both X-rays and radio. Apart from this, the orbital parameters of the system are not well known. Since the VHE γ-rays interact with the photons from the massive companion, mainly via γ-γ absorption, the emitted VHE light-curve depends on the orbital configuration. We created a Fortran code to compute the γ-γ absorption and simulate the emitted light-curve, assuming an intrinsic constant VHE flux, with different orbital parameters. Comparing our simulated results with H.E.S.S observations of 1FGL J1018.6−5856 we are able to fit the best possible parameters within the observation uncertainties, obtaining an eccentricity $e = 0.35 \pm 0.05$, an inclination $i = 42° \pm 5°$ and a periastron angle $w = 83° \pm 10°$. The results are coherent with the range of values suggested in the literature. However, these results are not in agreement if the GeV emission is only produced by anisotropic Inverse Compton scattering.

I. INTRODUCTION

A new type of binaries known as "gamma-ray binaries" have attracted a lot of interest in the last decade (Dubus 2013). Likewise other types of binaries such as X-ray or high energy (HE, 0.1–100 GeV), these very high energy (VHE, > 100 GeV) γ-ray binaries are formed by a neutron star or a black hole (from now on compact object) in orbit around a massive star (O,B). A non-thermal emission peak beyond 1 MeV in the spectral energy distribution is the characteristic marker of this new type of binaries. The production of γ-rays in these systems has been studied in the different compact object scenarios (Dubus 2015). The huge photon density around the massive star provides a large amount of optical photons ($E \sim$ eV) to produce both γ-ray emission due to Inverse Compton (IC) with HE and VHE electrons and γ-γ absorption with VHE γ-rays (more details in Section II).

Currently five γ-ray binary systems have been observed. Some of them have been carefully studied, such as LS 5039 and PSR B1259−63, the only one that has its compact object nature determined, being a 47.7 ms radio pulsar (see Dubus 2013 for a review). The object of our study is the γ-ray binary system 1FGL J1018.6−5856.

The system 1FGL J1018.6−5856 was discovered at GeV energies on a blind search for periodic sources in the Fermi-LAT data (Fermi LAT Collaboration et al. 2012). The position of the binary system is coincident with HESS J1018−589 A, which is part of a complex VHE γ-ray source together with HESS J1018−589 B (H.E.S.S. Collaboration et al. 2012). Optical observations show that the position of 1FGL J1018.6−5856 is coherent with the observation of a massive star of spectral type O6V((f)) (Fermi LAT Collaboration et al. 2012). A modulation of radio and X-ray flux with the same period of 16.58 days is observed (Fermi LAT Collaboration et al.

2012 and An et al. 2013) and taken as the orbital period of the system. The other orbital parameters are not well known, but eccentricity and inclination have been suggested to be small (H.E.S.S. Collaboration et al. 2015).

The goal of this work is to simulate the VHE emission light-curves of 1FGL J1018.6−5856 using different orbital parameters and compare the results with the H.E.S.S. observations of this γ-ray binary system. We start with a description of the γ-γ absorption and the Fortran code used to compute it. We continue with an in-depth analysis of the system 1FGL J1018.6−5856 observations focusing on the VHE emission. Afterwards we vary the possible orbital parameters (e, i and w), thus producing different light-curves assuming an intrinsic constant flux to find the orbital parameters that fit the light-curve. We finish with a discussion of the adjusted parameters and the incoherence we find with the GeV emission if it is only produced by anisotropic Inverse Compton scattering.

II. GAMMA-RAY ABSORPTION OPACITY

Considering a point-like star, the differential opacity observed by a γ-ray traveling along the direction $\vec{e}_\gamma$ interacting with a stellar photon with energy ϵ traveling along $\vec{e}_\star$, following Dubus (2006), is (see Fig. 1)

$$d\tau_{\gamma\gamma} = \pi \left(\frac{R_\star}{d} \right)^2 (1 - \vec{e}_\gamma \cdot \vec{e}_\star)\, \sigma_{\gamma\gamma} n_\epsilon \, dl \, d\epsilon, \qquad (1)$$

being $\vec{e}_\gamma$ and $\vec{e}_\star$ the photon unitary paths, $R_\star$ the star radius and d the distance between the star and the interaction point.

Applying our system geometry it is easily found (see Fig. 1)

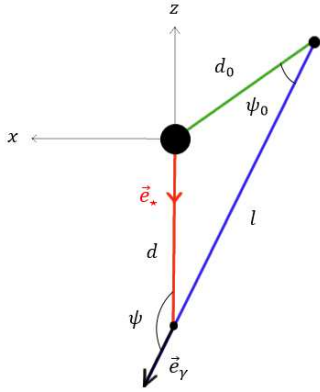$$1 - \vec{e}_\gamma \cdot \vec{e}_\star = 1 + \cos\psi \qquad (2)$$

FIG. 1: Geometric representation of the γ-γ absorption by a γ-ray and a stellar photon coming from the supposed point-like star. The x-z plane is given by the γ-ray ($\vec{e}_\gamma$) and stellar photon ($\vec{e}_\star$) directions. The length of the stellar photon path is d and the one of the γ-ray is l. The distance between the compact object and the point-like star is d_0.

The energy distribution of the stellar photons n_ϵ is taken as a blackbody radiation density with temperature $T_\star$:

$$n_\epsilon = \frac{2\epsilon^2}{(hc)^3}\cdot\frac{1}{\exp(\epsilon/\kappa T_\star)-1} \ \ \text{ph cm}^{-3} \text{ erg}^{-1} \text{ sr}^{-1}. \quad (3)$$

The photon-photon cross-section $\sigma_{\gamma\gamma}$ is given by Gould & Schréder (1967):

$$\sigma_{\gamma\gamma} = \frac{1}{2}\pi r_0^2(1-\beta^2)[(3-\beta^4)\ln\frac{1+\beta}{1-\beta} - 2\beta(2-\beta^2)] \quad (4)$$

where r_0^2 is the classical radius of the electron defined as $r_0 = e^2/mc^2$, the adimensional β parameter is written as $\beta = \sqrt{1-1/s}$ and s is

$$s = \frac{\epsilon E}{2m_e^2 c^4}(1 - \vec{e}_\gamma\cdot\vec{e}_\star) \quad (5)$$

being E the γ-ray energy and ϵ the stellar photon energy. If we take a closer look onto the s-variable and its effect onto β, and therefore onto $\sigma_{\gamma\gamma}$, there will only be interaction between the γ-ray and the stellar photon if $s \geq 1$, thus obtaining a threshold:

$$\epsilon E \geq \frac{2m_e^2 c^4}{(1+\cos\psi)} \quad (6)$$

The distance d is related to l, the distance between the γ-ray creation point and the interaction point, by the law of cosines:

$$d^2 = l^2 + d_0^2 - 2ld_0\cos\psi_0 \quad (7)$$

where ψ_0 is the corresponding angle, shown in Fig. (1), and d_0 is the distance between the massive star and the compact object both given by the orbit:

$$\cos\psi_0 = \sin(\theta + w)\cdot\sin i \quad (8)$$

where i is the inclination of the orbit, θ the orbit true anomaly and w the periastron angle.

The distance l is related to ψ by:

$$\psi = \tan^{-1}\left(\frac{d_0\sin\psi_0}{d_0\cos\psi_0 - l}\right) \ \text{ if } \ l < d_0\cos\psi_0 \quad (9)$$

$$\psi = \pi + \tan^{-1}\left(\frac{d_0\sin\psi_0}{d_0\cos\psi_0 - l}\right) \ \text{ if } \ l > d_0\cos\psi_0 \quad (10)$$

The dependence of the absorption opacity, $\tau_{\gamma\gamma}$, with its variables is explicit. Therefore, we can integrate for every possible l and photon stellar energy, ϵ.

$$\tau_{\gamma\gamma} = \int_0^\infty \int_{\epsilon_m}^\infty \frac{d\tau_{\gamma\gamma}}{dl\,d\epsilon} \ dl \ d\epsilon \quad (11)$$

being ϵ_m the threshold for interaction for a γ-ray with energy E

$$\epsilon_m = \frac{2m_e^2 c^4}{(1+\cos\psi)}\cdot E \quad (12)$$

The computation of the absorption opacity is shown to be non-trivial. Therefore we created a Fortran code to compute the absorption opacity by numerical integration using the point-like star approximation. To facilitate the numerical computation some adjustments have been made. As we can see in Eq. (11) our upper integral limits diverge, thus producing numerical problems when doing the computation. A change of variables has been done to circumvent the mentioned issue. We shall rewrite l and ϵ in terms of $\psi \in [\psi_0, \pi]$ and $\beta \in [0, 1]$ and integrate over them instead. Its differentials are:

$$dl = \frac{d_0\sin\psi_0}{\tan^2\psi \ \cos^2\psi}d\psi \quad (13)$$

$$d\epsilon = \frac{4m^2 c^4\beta}{E\,(1-\beta^2)^2\,(1+\cos\psi)} \ d\beta \quad (14)$$

As a sanity check a computation using our Fortran code has been made for the binary system LS 5039. A comparison with the results shown in Dubus (2006) for an extended star reveals a good agreement.

III. MULTIWAVELENGTH EMISSION OF 1FGL J1018.6−5856

The High Energy Stereoscopic System (H.E.S.S) is an array of imaging atmospheric Cherenkov telescopes located near the Gambsberg mountain, 100 km south-west of Windhoek, capital of Namibia. On Summer 2003 H.E.S.S. Phase I (H.E.S.S−I) became active with four Cherenkov telescopes. As of July 2012 a fifth telescope became operative. It is larger than the previous ones allowing for a better energy coverage. This event marked the start of H.E.S.S Phase II (H.E.S.S−II).

H.E.S.S–I observed the Carina arm region as part of the Galactic Plane Survey for five years starting in 2004.
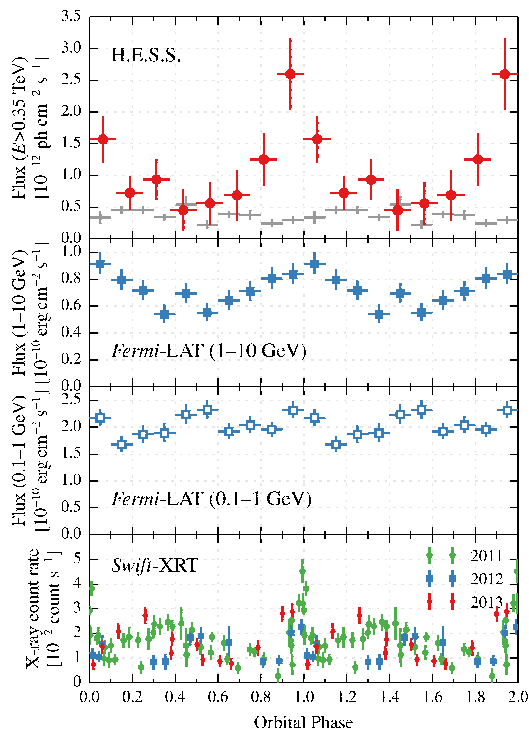
FIG. 2: Fluxes of 1FGL J1018.6−5856 folded with the orbital period of 16.58 d. Top: VHE integral flux above 0.35 TeV measured by H.E.S.S. (red circles); scaled lightcurve from the nearby source HESS J1023−589 (gray crosses). Middle top: Fermi-LAT lightcurve between 1 and 10 GeV (solid blue squares). Middle bottom: between 0.1 and 1 GeV (open blue squares; Fermi LAT Collaboration et al. 2012). Bottom: X-ray 0.3-10 keV count rate light-curve from 67 Swift-XRT observations in 2011 (green), 2012 (blue), and 2013 (red). In all cases the errorbars represent 1σ uncertainties. Figure from H.E.S.S. Collaboration et al. (2015)

.

H.E.S.S. Collaboration et al. (2012) presented a data set of 40h that was increased during the years to nearly 65h, focusing on the orbital phases whose HE and X-ray emission were maximum (H.E.S.S. Collaboration et al. 2015). The zenith angle of the observations was such that the mean energy threshold was of 0.35 TeV. This extended data set concurs with H.E.S.S. Collaboration et al. (2012) on the confirmation of a point-like VHE γ-ray emission, giving more weight to a point-like source separated from HESS J1018-589 B.

The H.E.S.S.–I data were folded with the 16.58 day orbital period using the reference time of $T_{\mathrm{max}} = \mathrm{MJD}$ 55403.3, corresponding to the maximum of GeV emission, as phase 0.0 (Fig. 2). The binning was chosen to have a significance of at least 1σ for each phase bin (see Fig. 2, from H.E.S.S. Collaboration et al. 2015).

A periodic TeV emission can be seen with a single peak per period near phase 0.95, and a rather wide minimum near phase 0.45 (Fig. 2, top panel, red circles). A supposedly constant bright γ-ray source (HESS

J1023−589) is shown for comparison. The 1–10 GeV emission from *Fermi*-LAT observations (Fig. 2, middle top panel) presents a periodic quasi-sinusoidal behavior with a maximum per period. For the 0.1–1 GeV emission from *Fermi*-LAT observations (Fig. 2, middle bottom panel), a roughly constant behavior of the flux is seen around 2×10^{-10} erg cm^{-2} s^{-1}. For the X-ray energies via *Swift*-XRT (Fig. 2, bottom panel), presented in both Fermi LAT Collaboration et al. (2012) and An et al. (2013), a periodic emission with a peak at phase 0.0 and a wide maximum between phase 0.1–0.8, depending on the orbital cycle, is clearly seen. In summary, for TeV, 1–10 GeV and X-ray emission a clear peak is observed around phase 0.95–0.00, although the shape of the light-curve is different in each energy band.

IV. SIMULATED TEV LIGHT-CURVES OF 1FGL J1018.6−5856

Assuming a constant intrinsic TeV flux for the source, the amount of γ-γ absorption depends on the orbital configuration and the orbital phase, resulting in a light-curve with a variable flux. The goal is to simulate the observed TeV light-curve of 1FGL J1018.6−5856 with our Fortran code using different values of the unknown orbital parameters: eccentricity e, inclination i and the periastron angle w. Considering the observational HESS light-curve for $E > 0.35$ TeV, an energy of 1 TeV is taken for the computation of the absorption.

The amount of possible variations of the orbital parameters would make the analysis very complex. Therefore, a variation of a single parameter is done while the others remain constant (Figs. 3, 4 and 5). Thus we make a grid of representative cases. First, an exploration of the parametric space is done to find simulated light-curves that are similar to the observed one, and to understand the variation of the light-curves depending on the different parameters. Second, a reference value is taken for each one of the parameters: being $e = 0.37$, $i = 45°$ and $w = 90°$. Third, a grid is done taking inferior and superior values of each reference parameter (range). A periastron $\phi_{\mathrm{peri}} = 0.935$ is used in every following figure (see discussion below). We shall keep in mind the already mentioned 1σ uncertainties of the observed light-curve and the intrinsically constant flux hypothesis.

In the following subsections we conduct a study of the influence of each parameter (e, i and w) and finally a fit to the best possible parameter configuration is done.

A. Variations of e, i and w

The HESS observational data can be reproduced with eccentricities in the range of $e = 0.2$–0.45 (e-range) (see Fig. 3). A minimum at phase 0.45 and a maximum at phase 0.95 can be seen in both light-curves. The lower eccentricity produces a more symmetric maximum and
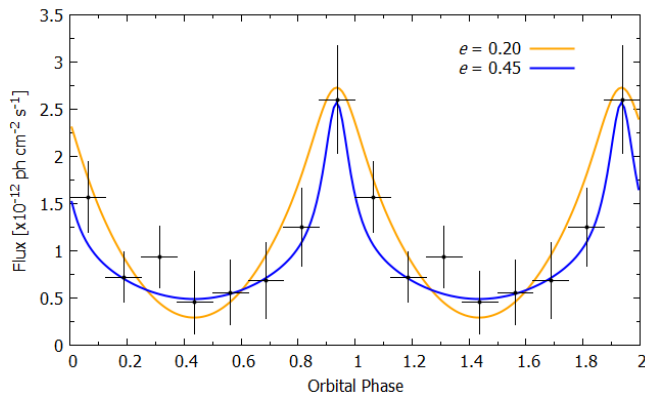
FIG. 3: Simulated light-curves of 1FGL J1018.6−5856 at 1 TeV obtained assuming a constant intrinsic flux and γ-γ absorption. The parameters used are: $e = 0.20$ (orange line) and $e = 0.45$ (blue line) for $i = 45°$ and $w = 90°$. The HESS observational data (dots) with their corresponding 1σ uncertainties are also included.
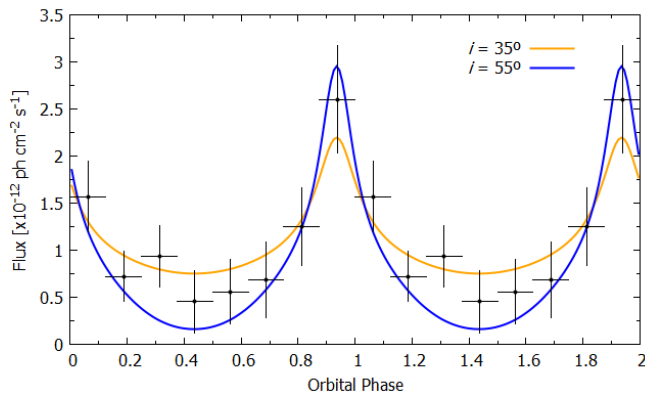

FIG. 4: Same as Fig. (3) with parameters: $i = 35°$ (orange line) and $i = 55°$ (blue line) for $e = 0.37$ and $w = 90°$.

minimum (Fig. 3, orange line) whereas the higher eccentricity produces a wider minimum and a sharper maximum (Fig. 3), blue line). The lower eccentricity also produces a greater maximum to minimum flux ratio. It is clear that a value in-between the e-range concurs with the observational HESS data.

Analyzing the inclination, the i value is within the range of 35°–55° (Fig. 4). A decrease of i produces a lower maximum to minimum flux ratio; also the minimum near phase 0.45 widens (see Fig. 4, orange line).

The last variable to analyze is the periastron angle w. Unlike e and i, the w parameter affects the mirror symmetry at phase 0.95 but does not affect the maximum to minimum flux ratio. As clearly seen in Fig. (5) (blue and orange lines) a variation from reference $w = 90°$ produces a difference on the slope before and after the maximum at phase 0.95, thus breaking the mirror symmetry. Take $w = 70°$ (Fig. 5 orange line) the slope around phase 0.1 is lower than the absolute value of the slope at phase 0.8.
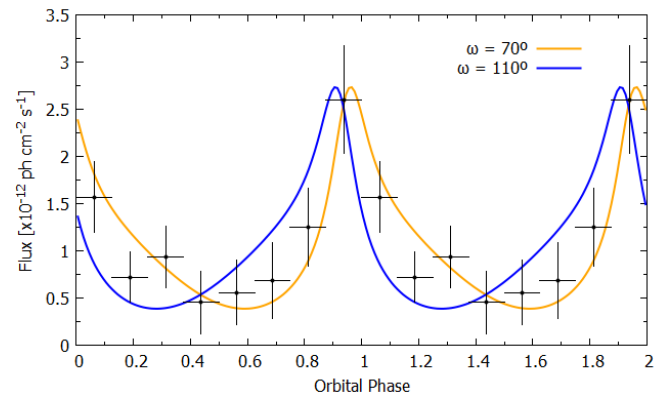

FIG. 5: Same as Fig. (3) with parameters: $w = 70°$ (orange line) and $w = 110°$ (blue line) for $e = 0.37$ and $i = 45°$.

B. Best-fit parameters

The behavior of the simulated light-curves of 1FGL J1018.6−5856 VHE flux is modulated via all three orbital parameters. Therefore, possible values of the system orbital parameters can be obtained with a fitting process: $e = 0.35 \pm 0.05$, $i = 42° \pm 5°$ and $w = 83° \pm 10°$ (Fig. 6). Each parameter has a 1σ uncertainty, keeping the other parameters constant. To obtain the best possible fit we have imposed the periastron phase at $\phi_{\mathrm{peri}} = 0.935$.

Both i and e act upon the maximum to minimum flux ratio. The eccentricity also acts on the ratio between the widths of the maximum and minimum. In our system the observational data indicates a rather small difference between the width of the maximum and minimum, the minimum being wider than the maximum. This indicates a small eccentricity as suggested by H.E.S.S. Collaboration et al. (2015). The w parameter is the most difficult one to constrain due to the uncertainties of the HESS data. However, given the slight difference in slopes around phase 0.95 a periastron angle of $w = 83°$ is fit.

We obtain a maximum flux at the inferior conjunction with $\phi = 0.945$, thus a minimum of pair production when the compact object is in front of the massive star (see Fig. 7). This is consistent with Strader et al. (2015).

It is interesting to note that the TeV and 1–10 GeV light-curves maxima are at similar orbital phases (see Fig. 2). This fact is at odds with the anisotropic IC scattering that should dominate at GeV energies and whose maximum should be at the superior conjunction, near phase 0.45, because the collisions are more face-on.

V. CONCLUSIONS

In γ-ray binary systems, VHE γ-rays coming from the compact object can interact with photons of the massive star thus resulting in pair production (creation of electrons and positrons). Thus, a binary system emitting VHE γ-rays experiences a modulation of this mentioned

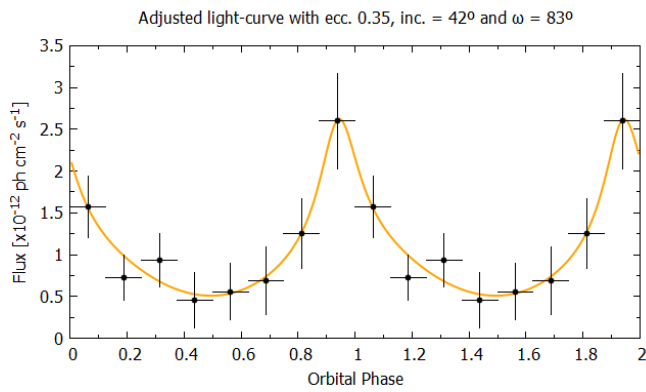FIG. 6: Same as Fig. (3) with the best-fit parameters $e = 0.35$, $i = 42°$ and $w = 83°$.

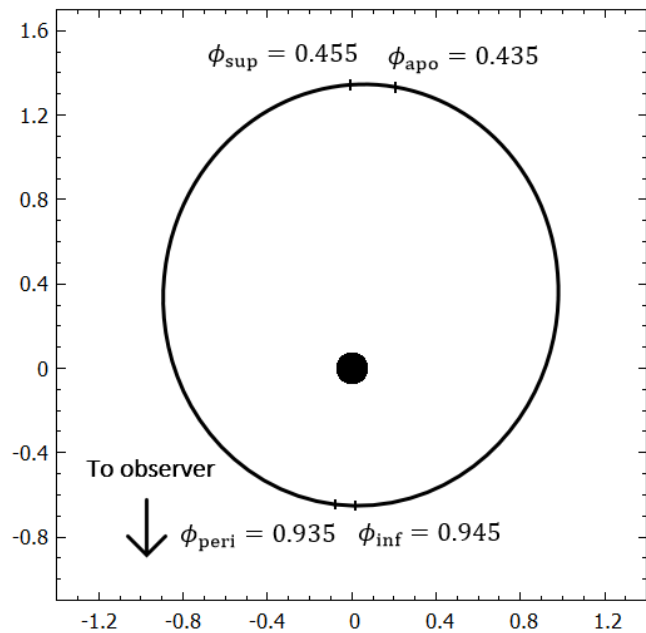FIG. 7: Representation of FGL J1018.6−5856 orbit with $e = 0.35$, $i = 42°$ and $w = 83°$ but seen from above ($i = 0°$). The $\phi_{\text{peri}} = 0.935$ corresponds to the periastron, $\phi_{\text{apo}} = 0.455$ to the apastron, $\phi_{\text{inf}} = 0.945$ to the inferior conjunction and $\phi_{\text{sup}} = 0.455$ to the superior conjunction. The axis are represented in semimajor axis units.

interaction (absorption). This process is well enough understood to be able to do computer simulations of the possible results given the system orbital geometry. We have written a Fortran code to compute the mentioned modulated absorption depending on the orbital configuration and compared it with the observational data of 1FGL J1018.6−5856 obtained with H.E.S.S−I. A point-like star approximation is taken and the hypothesis of an intrinsic constant flux is done.

Since the orbital parameters of 1FGL J1018.6−5856 are not well known, a grid of possible orbital configurations is done to fit them. The observational H.E.S.S data can be fit with a simulated light-curve with parameters: eccentricity $e = 0.35 \pm 0.05$, inclination $i = 42° \pm 5°$ and periastron angle $w = 83° \pm 10°$ (see Fig. 6).

The relatively low eccentricity and inclination, for a γ-ray binary, obtained is consistent with H.E.S.S. Collaboration et al. (2015). Also, the maximum flux being in the inferior conjunction is in agreement with Strader et al. (2015). When comparing the multiwavelength emission of 1FGL J1018.6−5856 (Fig. 2) with our parametric results an inconsistency emerges. If the GeV emission is only produced by anisotropic IC scattering the maximum flux should be at the superior conjunction, because the collisions are more face-on. This fact clashes with the HESS observational data where the GeV maximum is at the inferior conjunction like the TeV maximum. The discrepancy indicates a more complex problem than the one proposed, and surely the influence of other phenomena such as variable particle acceleration along the orbit or cascading effects.

Moreover, the data uncertainties of 1σ are not conclusive to pin-point the exact parameter values and further observations of the system should provide of a better understanding. Our results though, coincide with the current literature values for the orbital parameters of 1FGL J1018.6−5856.

Acknowledgments

An, H., Dufour, F., Kaspi, V. M., & Harrison, F. A. 2013, Astrophys. J. , 775, 13
Dubus, G. 2006, A&A, 451, 9
Dubus, G. 2013, A&A, 21, 64
Dubus, G. 2015, Comptes Rendus Physique, 16, 661
Fermi LAT Collaboration, Ackermann, M., Ajello, M., et al. 2012, Science, 335, 189
Gould, R. J., & Schréder, G. P. 1967, Phys. Rev., 155, 1404

H. E. S. S. Collaboration, Abramowski, A., Acero, F., Aharonian, F., et al. 2012, A&A, 541, A5
H. E. S. S. Collaboration, Abramowski, A., Aharonian, F., et al. 2015, A&A, 577, A131
Strader, J., Chomiuk, L., Cheung, C. C., Salinas, R., & Peacock, M. 2015, ApJ, 813, L26